Advances in Water Resources 33 (2010) 801–812

Contents lists available at ScienceDirect

Advances in Water Resources

journal homepage: www.elsevier.com/ locate/advwatres

Stochastic evaluation of subsurface contaminant discharges under physical, chemical, and biological heterogeneities

M. Mohamed [a,b,*], K. Hatfield [c], A. Hassan [b], H. Klammler [c,d]

[a] Civil and Environmental Engineering Department, United Arab Emirates University, P.O. Box 17555, Alain, United Arab Emirates
[b] Irrigation and Hydraulics Department, Faculty of Engineering, Cairo University, P.O. Box 12211, Giza 12613, Egypt
[c] Civil and Coastal Engineering Department, University of Florida, P.O. Box 116580, Gainesville, FL 32611, USA
[d] Department of Environmental Science and Sustainable Development, Federal University of Bahia, Barreiras, Bahia, Brazil

ARTICLE INFO

Article history:
Received 31 August 2009
Received in revised form 11 April 2010
Accepted 14 April 2010
Available online 6 May 2010

Keywords:
Monte Carlo
Mass discharge
Groundwater
Biodegradation

ABSTRACT

A finite element 2D Monte Carlo approach is used to evaluate the sensitivity of groundwater contaminant discharges to a Damkohler number ω and spatial variability in aquifer hydraulic conductivity, initial microbial biomass concentrations, and electron acceptor/donor concentrations. Bioattenuation is most sensitive to spatial variations in incipient biomass and critical electron donors/acceptors for $\omega \geq 1$ (i.e., when pore-water residence times are high compared to the time needed for microbial growth or contaminant attenuation). Under these conditions, critical reaction processes can become substrate-limited at multiple locations throughout the aquifer; which in turn increases expected contaminant discharges and their uncertainties at monitored transects. For $\omega \leq 0.2$, contaminant discharge is not sensitive to incipient biomass variations. Physical heterogeneities expedite plume arrival and delay departure at transects and in turn attenuate peak discharges but do not affect cumulative contaminant discharges. Physical heterogeneities do, however, induce transect mass discharge variances that are bimodal functions of time; the first peak beings consistently higher. A simple stream tube model is invoked to explain the occurrence of peaks in contaminant discharge variance.

1. Introduction

Estimation of subsurface contaminant mass discharge (i.e., contaminant mass per unit time) at specified control planes (CPs) is an effective approach of defining groundwater source terms and boundary conditions; assessing natural attenuation viability; designing time-effective enhanced remediation systems; and evaluating source zone remediation success [1–4]. Traditional estimations of contaminant mass discharges using collected groundwater samples are inaccurate because they ignore spatial variations in both concentrations and groundwater flows [5]. Direct measurements of groundwater and contaminant discharges, which accounts for spatial variations of contaminant concentrations and discharges, are possible through the deployment of Passive Flux Meters (PFM) [1,6–9]; and improved analyses of the Integral Pumping Test (IPT) approach [10–15]. As a partial consequence of improved flux monitoring, several investigators have used or proposed to use measured reductions in contaminant discharge as an indicator of contaminant source mass depletion [1,16–28].

Various types of heterogeneities have been reported to affect contaminant fate and transport, and therefore discharge in the subsurface including physical, chemical, and biological heterogeneities [e.g. 29–37]. The relationship between source mass and CP discharge is a function of these heterogeneities and the correlation between them [1,16,19,22,23]. Physical aquifer heterogeneity, represented by spatial variability in hydraulic conductivity, has been studied extensively to characterize field-scale dispersion [e.g. 29–34]. A typical manifestation of this heterogeneity is the apparent presence of anisotropy at the aquifer scale, despite point scale observations of isotropic hydraulic conductivities [30,38]. Another intensively investigated manifestation of physical heterogeneity is macro-dispersion [33,34,39–42]. Chemical heterogeneity in the subsurface is represented as spatial variability in abiotic contaminant reaction parameters including abiotic degradation rates; sorption coefficients and redox conditions and spatial variability in electron donor/acceptor concentrations that are critical for biotic reactions [35–37,43–47]. Chemical heterogeneity in the aquifer matrix has been recognized at laboratory scale [48–52], and at field scale [44,53]. Finally, biological heterogeneity is manifested as spatial variability in microbial species, biomass, and microbial activity. Several stochastic modeling techniques have been used to examine organic subsurface biodegradation at the field scale [54,55]. Monte Carlo simulations were used to study the effects of spatially distributed rates of biodegradation and hydraulic

* Corresponding author. Civil and Environmental Engineering Department, United Arab Emirates University, P.O. Box 17555, Alain, United Arab Emirates. Tel.: +971 3 7133509.
E-mail address: m.mohamed@uaeu.ac.ae (M. Mohamed).

0309-1708/$ – see front matter © 2010 Elsevier Ltd. All rights reserved.
doi:10.1016/j.advwatres.2010.04.010

conductivity on plume-scale rates of biodegradation [56–58]. They were also used for assessing the effects of waste sites on groundwater quality [59–62].

Accounting for spatial variability is particularly essential for accurate estimation of subsurface contaminant mass discharges and thus successful remedial design [15]. The effect of spatially variable hydraulic conductivity on the variances of both the contaminant concentrations and discharges has been studied analytically for solutes undergoing first-order sorption kinetics under pulse or continuous injections of concentrations from source zones [63–65]. However, the effect of biological variability, correlation between spatial hydraulic conductivity and biological variability, and electron donor/acceptor availability on contaminant mass discharges has not been examined to the best of the authors' knowledge. Zones with high contaminant discharge may have different microbial activity than low-discharge zones, which would impact plume remedial design that is based on enhancement of biological processes [1].

The objective of this paper is to examine the sensitivity of microbial mediated contaminant mass discharges to physical, chemical, and biological heterogeneities in a 2-dimensional aquifer. Monte Carlo simulations are used to simulate contaminant plumes in a two-dimensional aquifer, and at two sections transverse to the mean groundwater flow direction, and generate temporal distributions of the mean subsurface contaminant discharge and variance. One can legitimately argue than two-dimensional simulations are poor approximations to natural three-dimensional systems. However, two-dimensional models are of value when studying problems at the regional scale [7]. The regional scale is defined for aquifers whose planar dimension is much larger than the aquifer thickness. In this case formation properties are averaged over depth and are regarded as functions of the horizontal dimension only [66]. Steady, uniform, and two-dimensional flow prevails at the natural gradient tracer experiment in the sand aquifer that was carried out at the Borden site [67–69]. Freyberg [69] found that the motion of the plume and its center of mass is essentially horizontal. Barry et al. [70] also found the assumption of two-dimensional flow to yield good results. In the other commonly cited natural tracer test, performed at the Cape Cod site, LeBlanc et al. [71] found that the plume centroid moved vertically downward for a small distance which enabled Deng et al. [72] to reproduce the field spatial moments using a two-dimensional stochastic model. Chaudhuri and Sekhar [61] performed 1D Monte Carlo Simulations (MCS) to evaluate a perturbation technique. Then, they used this technique on 3D simulations. They concluded that 100 realizations were not enough to obtain good MCS results in 3D simulations. This is an added difficulty of simulating 3D with MCS. The induced variations in plume discharge are the result of spatial heterogeneities in aquifer hydraulic conductivity, microbial biomass concentrations, and electron donor/acceptor concentrations. Microbial growth is simulated using modified Monod kinetics [73] under conditions where microbial growth will be substrate-limited depending on the local concentrations of contaminant and an auxiliary electron acceptor/donor.

2. Governing equations

One of the challenges in modeling biotransformation is obtaining reliable conceptual description. Molz et al. [74], separated biodegradation models into three distinct conceptual approaches. In the first approach, it is assumed that solid particles are uniformly covered by a thin biofilm [57,75–85]. Consumption of contaminants occurs in this biofilm in the presence of electron acceptors and nutrients. This approach will be employed in this paper. In the second approach, bacteria are assumed to grow, in small discrete colonies (or 'micro-colonies') attached to a particle surface, as the result of substrate and electron acceptor utilization [86,87]. Both biofilm and micro-colony approaches employ one of the following three reaction kinetics: first-order decay, instantaneous reaction kinetics, and multi-term Monod (or Michaelis–Menten) expressions. The third approach has been adopted by many researchers [88–93]. In this approach, partitioning between free flowing and adsorbed microorganisms is assumed [89,90] but their distribution and interaction play no role in depicting the growth dynamics [94].

For a heterogeneous porous medium, the time-dependent reaction–advection–dispersion equation of a contaminant (and/or electron donor/acceptor) (i) whose spatial concentration distribution is denoted by $C_i(x, t)$ is given by:

$$R_i \frac{\partial C_i}{\partial t} = \frac{\partial}{\partial x}\left(D\frac{\partial C_i}{\partial x}\right) - V\frac{\partial C_i}{\partial x} + Q_i^{\text{bio}} \tag{1}$$

where the local pore-water velocity vector is V [$\mathrm{L\,T^{-1}}$]; D [$\mathrm{L^2\,T^{-1}}$] is the tensor of the hydrodynamic dispersion coefficient, and R is the retardation factor [dimensionless]. For multi-solute transport (electron acceptors/donors, and/or nutrients), these equations are coupled through contaminant source/sink terms Q as follows:

$$Q_i^{\text{bio}} = \frac{-M\mu}{Y_i\theta} \tag{2}$$

where M is the microbial biomass concentration [$\mathrm{M\,L^{-3}}$], θ is the aquifer porosity [dimensionless], Y_i are the yield coefficients [dimensionless] representing the mass of bacterial species produced per unit mass of electron donor/acceptor. Modified Monod kinetics [73] is used to describe specific growth rate of the microbial species utilizing electron donor and electron acceptor:

$$\mu = \mu_{\max}\prod\left(\frac{C_i}{\left(K_{C_i} + C_i\right)}\right) \tag{3}$$

where $\mu_{\max}$ is the maximum specific growth rate for the microbial species [$\mathrm{T^{-1}}$], K_{C_i} is the half saturation coefficient for the electron donor/acceptor [$\mathrm{M\,L^{-3}}$]. Assuming B as the first-order microbial decay rate, the microbial mass balance equation can be written as follows [95,96]:

$$\frac{dM}{dt} = M(\mu - B). \tag{4}$$

3. Methodology and problem description

Monte Carlo (MC) simulations are used in this study to investigate spatial–temporal variations in subsurface microbial mediated contaminant discharge affected by a Damkohler number ω and physical, chemical, and biologically heterogeneities in a 2-D aquifer. Physical heterogeneity is represented as spatial variations in hydraulic conductivity. Biological heterogeneity is manifested as spatial variations in initial and transient distributions of microbial biomass, and finally chemical heterogeneity is represented as spatial variations in the concentration of a requisite electron donor/acceptor. Monte Carlo simulations provide predictions for ensemble mean discharges at transects as well as the uncertainty in these predictions represented as discharge variances. Comparisons between Monte Carlo simulations and corresponding homogeneous scenarios of assumed uniform physical, chemical, and biological properties is used to elucidate the effects of physical, chemical, and biological heterogeneities and their possible correlation on contaminant mass discharges. Quantifying the uncertainty of the prediction has been recognized as crucial information for remediation design and risk assessment studies [97,98].

The methodology used here is as follows: (1) a random field generator (RFG) [99,100] is used to create multiple realizations of spatially varying fields of aquifer hydraulic conductivity and initial concentrations of a requisite electron donor/acceptor and biomass assuming a known spatial correlation structure of second-order stationarity. The method used in this RFG is based on Fast Fourier Transform (FFT) and is chosen in this study because of its computational efficiency. The basic concept of this method is to generate a set of uniformly distributed random numbers by using a random number generator. By taking the FFT of these numbers, the resulting spectrum will have a uniform density of unity. By multiplying the transformed numbers by the square root of the spectral density function of the conductivity field (the Fourier transform of ln K covariance), the resulting numbers will have the same spectrum as that of the hydraulic conductivity field. Finally taking the inverse FFT of those numbers gives a set of numbers in real space having the same correlation structure as that of the conductivity field; (2) the groundwater flow is established for all conductivity realizations under the specified boundary conditions (Fig. 1); (3) the finite element model METABIOTRANS [57,101,102] is used to solve the coupled transport equations and microbial growth equation (Eqs. (1)–(4)); (4) contaminant discharges at sections 1 and 2 (Fig. 1) are obtained from each realization; and finally (5) the ensemble mean discharge and discharge variance are calculated for all realizations.

The hydraulic conductivity, initial concentrations for the requisite electron donor/acceptor, and biomass are assumed to have a log-normal distribution with an exponential covariance structure ($\mathrm{Cov}(r)=\sigma^2 e^{-r/\lambda}$) in which σ^2 is the process variance, r is the spatial lag, and λ is the correlation length which is proportional to the distance over which hydraulic conductivity (K), the requisite initial electron donor/acceptor (A) concentration, or initial biomass (M) concentration are spatially correlated. The value of λ is kept as 1.0 m for all simulations. Depending on the simulation, it is assumed that Log K and Log A variances are both 1.0, Log M variance is 1.0 or 3.0, and the arithmetic mean for M equals 1% of C_o (initial concentration). The element size in the finite element mesh is a constant 0.2λ. Longitudinal and transverse dispersivities are assumed to be 0.1λ and 0.05λ, respectively. Summary of all input parameters used in this paper is presented in Table 1.

The log-normal distribution with exponential covariance structure is a common assumption in stochastic groundwater studies. In the same way as the Central Limit Theorem dictates that the sums of a large number of independent variables approaches a normal distribution it dictates (after exponentiation) that the product of a large number of independent (non-negative) variables approaches a log-normal distribution. This is known to be true even if partial correlation between variables is present; however, in this case convergence to (log-) normality is slowed down [106]. As illustrated by the governing equations, the processes studied here are purely multiplicative and limited to non-negative variables. Regarding the state of a variable as the outcome of a large number of such multiplicative but not necessarily uncorrelated processes (e.g., along a stream line in space or at a location over time) lends support to the assumption of log-normality for the respective variables. Moreover, we hypothesize that deviations from the log-normal distribution (e.g., towards other non-negative distributions such as gamma, chi-squared, etc.) may have some quantitative but no significant qualitative impact on simulation results and conclusions as long as mean and variance remain unaffected.

Table 1
Summary of input parameters.

Problem domain	36λ × 18λ
Element size in X-direction ($\Delta x/\lambda$)	0.2
Element size in Y-direction ($\Delta y/\lambda$)	0.2
Dispersivity in X-direction (α_x/λ)	0.1
Dispersivity in Y-direction (α_y/λ)	0.05
Porosity (n)	0.3
Retardation factor (R)	1.0
Half saturation coefficient for ED (K_s/C_o)	0.4 [103,104]
Half saturation coefficient for EA (K_a/C_o)	0.4 [103,104]
B/μ_{max}	0.1 [104,105]
Size of the contamination initial source	4λ × 2λ

In the case of the spatial covariance model chosen, we argue that deviations from the exponential model (e.g., towards other stationary models such as spherical, Gaussian, etc.) do not have a significant impact on results as long as the correlation length remains unaffected and the spatial scale of the study (i.e., transect size over which local fluxes are added up to determine discharges) exceeds the correlation length by some factor. Under these conditions it is assured that some "average" level of correlation between different locations within the model domain is maintained, which determines the overall behavior of the (spatially-averaged or integrated) outcome. From this we hypothesize that results presented retain approximate quantitative and general qualitative validity for the set of fundamental parameters mean, variance and correlation length and independent of particular distributional or spatial covariance properties. This is consistent with the level of information that may typically be expected in field situations (limited data may not even allow for making strong inferences about distributions or spatial correlation structures).

Field measurements revealed that the spatially varying hydraulic conductivity could be described by a log-normal distribution. Furthermore, conductivity values were found to be spatially correlated with a correlation structure that varies from site to site. The exponential, Gaussian, hole-type, and fractal covariance structures are among the commonly used covariances. Examples of studies that employed the exponential model include Mohamed et al. [57] and Hassan et al. [92,93]. The latter is assumed to also apply to biomass and electron donors in the present work due to their correlation with

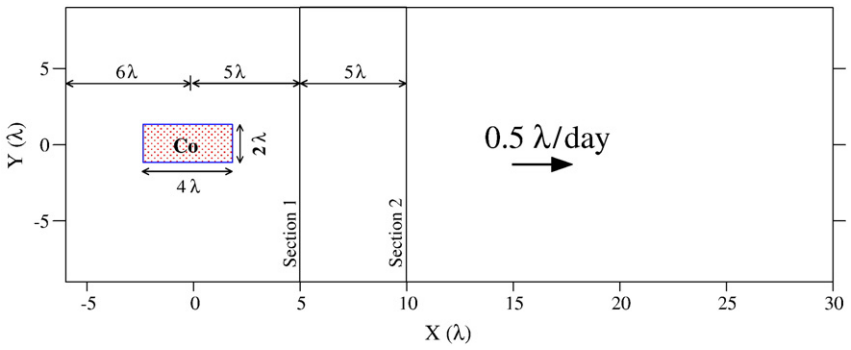

Fig. 1. Problem layout.

conductivity. For the case of no correlation we maintain the exponential variogram for better comparison.

Five different scenarios are used to study plume contaminant discharges under various conditions of spatial heterogeneity (Table 2). The first scenario includes three homogeneous simulations from which reference conditions are defined. The computational time of any of these deterministic simulations was 20.5 min on a 2 GHz machine. The next two scenarios examine separate influences of physical heterogeneity (hydraulic conductivity variations) and biological heterogeneity (spatial variations in initial microbial biomass concentrations). The fourth scenario focuses on the composite influence of correlated physical and microbial heterogeneities. In the final scenario, chemical heterogeneity is examined through a single MC simulation conducted with uncorrelated spatial variations in initial electron donor/acceptor concentrations, and spatially correlated variations in hydraulic conductivity and microbial biomass. Simulations include sensitivity studies on the assumed dimensionless microbial effective growth rate ($\omega = \lambda\mu_{max}/V$), and the assumed the initial biomass concentration variance. ω is equivalent to a Damkohler number [107,108], and it expresses the ratio of pore fluid hydraulic residence time to the time required for microbial growth and contaminant attenuation. Thus, $\omega \leq 1$ suggests contaminant attenuation may be sensitive to local variations in groundwater velocity. This sensitivity may arises because the characteristic maximum specific growth rate for the microbial population is sufficiently low, or groundwater velocities are sufficiently high that the time require for attenuation and microbial growth is significantly greater than the average groundwater hydraulic residence time. For a given μ_{max}, as the groundwater velocity decreases the hydraulic residence time increases; thus, ω increases indicating there is sufficient pore-water residence time to support microbial growth and contaminant attenuation. Based on available literature values for μ_{max}, the parameter ω can range from 0.001 to 64 [57].

In the three homogeneous simulations (1–3 from Table 2) ω varied from 0 to 1. Simulations results serve as references in subsequent comparisons with MC simulations. Background biomass concentrations in the first three simulations were equated to 1% of the initial contaminant concentrations (Co), which is within the range of 0.5–10% assumed in previous studies [e.g. 40,52,54]. To ensure meaningful comparisons between the homogenous simulations and those involving biological heterogeneities, this value of background biomass concentration is used to represent the mean biomass concentration in the Monte Carlo simulations presented in scenarios 2, 4, and 5. For the same reason and to ensure meaningful comparisons between the homogenous simulations and those involving physical heterogeneities, the geometric mean of the log-normal K equals the uniform hydraulic conductivity field in the simulations presented in scenarios 3–5. In addition, the same hydraulic gradient is used in all simulations to achieve the same integrated groundwater discharge at any transect in the flow domain (i.e. the same spatially-averaged specific discharge over any arbitrary transect draw perpendicular to the predominant flow direction).

Table 2
Summary of simulation parameters.

Scenario	Simulation	Number of realizations	Random variable	ω	Variance of K, M, and A
1	1	Homogenous	–	0	–
	2	Homogenous	–	0.2	–
	3	Homogenous	–	1.0	–
2	4	500	K	0	1.0
	5	500	K	0.2	1.0
	6	500	K	1.0	1.0
3	7	250	M	0.2	1.0
	8	250	M	1.0	1.0
	9	250	M	1.0	3.0
4	10	500	K and M (uncorrelated)	0.2	1.0 and 1.0
	11	500	K and M (negative correlation)	0.2	1.0 and 1.0
	12	500	K and M (uncorrelated)	1.0	1.0 and 1.0
	13	500	K and M (negative correlation)	1.0	1.0 and 1.0
	14	500	K and M (positive correlation)	1.0	1.0 and 1.0
	15	500	K and M (positive correlation)	1.0	1.0 and 3.0
5	16	500	K and M (negative correlation) and uncorrelated to A	1.0	1.0 and 1.0 and 1.0

Results of all simulations are shown as dimensionless graphs expressed in terms of the normalized time ($\tau = tV/\lambda$) and normalized ensemble mean contaminant mass discharge ($ND = Q/Q_{max}$); where Q is the actual mass discharge [$M\,T^{-1}$] and Q_{max} is the maximum mass discharge representing mass recharge when dispersion and biodegradation are ignored. The maximum mass discharge (Q_{max}) is equivalent to ($VM_r/4\lambda$); where M_r is the total initially released mass of the contaminant [M]. Discharges are evaluated at two sections located at distances 5λ and 10λ, respectively, downstream from the center of the initial contaminant release as presented in Fig. 1.

4. Numerical simulations and discussion

4.1. Physical heterogeneity

The effects of physical heterogeneity on plume contaminant discharge are examined through three MC simulations (4–6, Table 2). In all three, 500 realizations of the hydraulic conductivity field of unit log-variance are used to generate 500 heterogeneous velocity fields, which are then used in the transport model. Biodegradation is not simulated in 4 ($\omega = 0$); whereas in MC simulations 5 and 6, biological activity is simulated using values of ω comparable to homogeneous simulations 2 and 3 (i.e. 0.2 and 1.0), respectively (Table 2).

Physical heterogeneity increases dispersion in both longitudinal and transverse directions, which explains the early increase and the delayed decrease in ensemble mean contaminant discharges at each transect and in turn the attenuated peak discharges compared to homogeneous simulations (see Fig. 2a). Theses peaks occur at approximately the time when the centroid of the ensemble contaminant plume traverses the transect plane. However, this is not the case with mass discharge variance (DV). At any given transect, the DV produces two peaks over time corresponding to two periods of high uncertainty in mass discharge (Fig. 2b). The first peak is observed to be associated with the arrival of the leading edge of the ensemble plume (i.e., when the steepest increase in ND occurs), while the second occurs as the plume's trailing edge traverses the transect plane (i.e., when the steepest decrease in ND occurs).

A simple stream tube model with longitudinal and transverse dispersion between stream tubes can be invoked to explain the two peaks is discharge variance. First, it is assumed n [dimensionless] stream tubes of equal water flux crossing a control section and each stream tube either makes a contribution to mass discharge or not. At short times all contaminated stream tubes may be assumed to convey a mass flux q_{max} corresponding to some maximum (saturated) contaminant concentration. Next, it is assumed that the probability that a stream tube is contaminated is p [dimensionless] and to be clean $1-p$. The resulting distribution is known as Bernoulli distribution, which, after summation over n stream tubes, becomes a Binomial distribution of mean npq_{max} and variance $np(1-p)q_{max}^2$. By equating $ND = npq_{max}$ (expected mass discharge) Fig. 2a indicates that p rises from zero to some maximum value $p_{max} \leq 1$ and decreases towards zero afterwards. This reflects the effect of longitudinal dispersion and the lower probability of encountering contaminated stream tubes before and after the plume core. By further equating

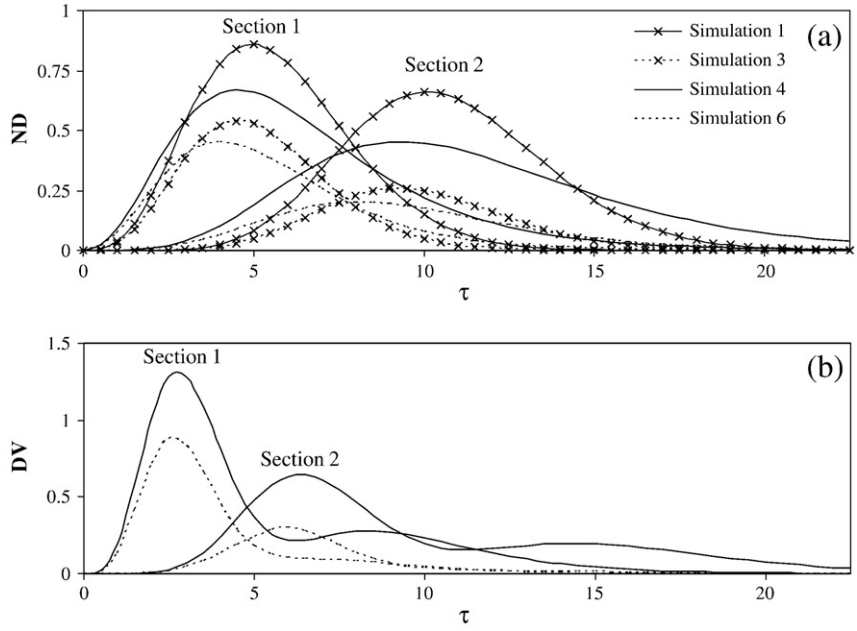

Fig. 2. Comparison between homogenous simulations [1($\omega = 0.0$) and 2($\omega = 0.2$)] and physical heterogeneity simulations [4 ($\omega = 0.0$) and 5 ($\omega = 0.2$)] (a) normalized mean discharge, and (b) discharge variance.

$DV = np(1-p)q_{max}^2$ and noting that $p(1-p)$ is a concave function equal to zero for $p = 0$ and 1 while reaching a maximum at $p = 0.5$, it is shown that DV possesses two maxima corresponding to p reaching 0.5 at the leading and trailing edges of the plume. From a different perspective these peaks can be related to the uncertainty in plume arrival/departure times and the magnitudes of the arriving and departing discharge gradients in flow direction. At very short and very large times p and, hence, DV are zero, while in between peaks $0.5 < p \leq p_{max}$ and DV reaches a local minimum. Now considering also transverse dispersion between stream tubes, which grows with the length of the flow path and time, stream tubes can convey arbitrary discharges q between zero and q_{max}. This does not directly affect ND, since transverse dispersion does not discriminate between faster and slower stream tubes (i.e., its effects on ND cancel out on average), but it does decrease DV, since individual stream tube discharges are moved closer to the mean value. This may explain the smaller amplitude of the second peak (trailing plume "fingers" are fuzzier than leading plume fingers) as well as of the peaks at the downgradient section 2. Cases may exist where this effect (possibly in combination with degradation) is strong enough to eliminate a second peak or where $p_{max} \leq 0.5$.

In the absence of biodegradation, time-integrated contaminant discharges must equate to the initial source mass. Results shown in Table 3 for simulations 1 and 4 verify this claim, and they also validate the numerical scheme used to integrate discharges at each section. Biodegradation decreases the time-integrated discharge between sequential transect planes; the magnitude of decrease is sensitive to ω but insensitive to spatial variations in hydraulic conductivity. For example, from a comparison of simulations 2 and 3 with 5 and 6 (see Table 3), essentially the same contaminant mass is observed to traverse respective transects at the levels of physically heterogeneity simulated in this study. It is important to keep in mind for these simulations; Monod parameters (Table 1) are spatially uniform. However, if these conditions were otherwise, biodegradation rates would vary spatially in accordance with spatial variation in Monod parameters.

Contaminant concentration reductions due to biodegradation decrease DV as a plume migrates through a transverse section. A closer look at the differences between simulations 4 and 5 in Fig. 2b suggests a greater relative decrease in DV occurs at the trailing edge of a simulated plume (second peak) than at the leading edge (first peak). This occurs most likely because the trailing edge encounter a higher density of active biomass produced as microbial growth increased to consume the leading edge of the plume, and also because the travel time and in turn the exposure to active microbial colonies is longer for contaminants in the trailing edge of plume. Increasing ω in simulation 6 increases significantly the contaminant mass degraded; however, it does not affect the arrival time of the leading edge of plumes in either homogenous or physically heterogeneous cases (compare Figs. 2a and 3a). Thus, q_{max} and contaminant DV decrease at both sections in simulation 6 (Fig. 3b), so much so that the second variance peak is almost negligible.

4.2. Biological heterogeneity

In this third scenario, variability in initial biomass concentrations is considered. Biological heterogeneity is represented in this paper by a spatial variability in the distribution of microbial species, biomass, and microbial activity. Though this is the least understood of the other factors of heterogeneity, spatial variations in biological processes are believed to have a significant effect on contaminant transport in the

Table 3
Ratios of cumulative contaminant mass discharges and total contaminant source mass for sections 1 and 2 at end of simulations ($\tau = 35$).

Simulation	Section 1	Section 2
1	1.00	1.00
2	0.90	0.81
3	0.63	0.39
4	1.00	1.00
5	0.88	0.81
6	0.62	0.40
7	0.90	0.82
8	0.66	0.42
9	0.70	0.46
10	0.88	0.81
11	0.89	0.81
12	0.65	0.44
13	0.65	0.44
14	0.65	0.43
15	0.71	0.51
16	0.87	0.77

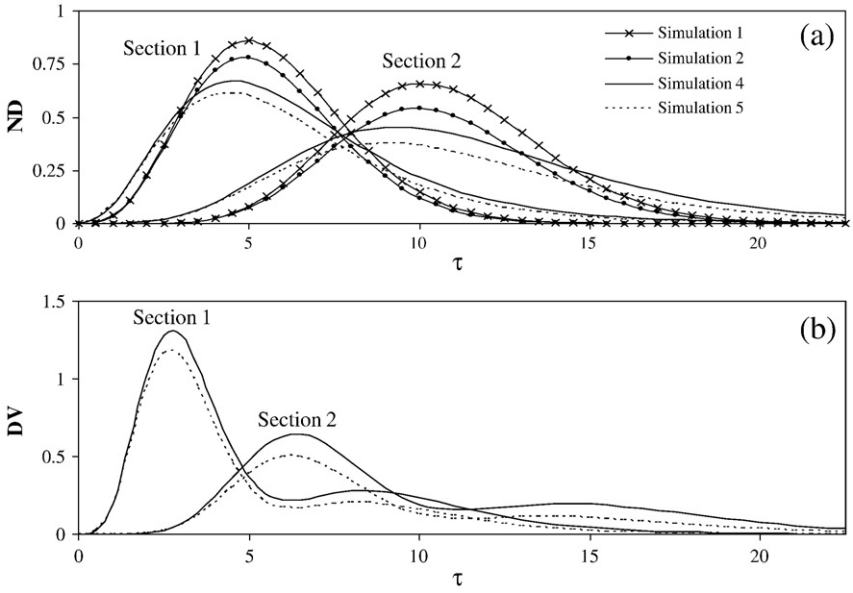

Fig. 3. Comparison between homogenous simulations [1($\omega = 0.0$) and 3($\omega = 1.0$)] and physical heterogeneity simulations [4($\omega = 0.0$) and 6($\omega = 1.0$)] (a) normalized mean discharge, and (b) discharge variance.

subsurface. Both Miralles-Wilhelm et al. [54,55] and Scholl [56] have used stochastic modeling techniques to examine organic subsurface biodegradation at the field scale. Miralles-Wilhelm et al. [54] presents an analytical model to quantify subsurface oxygen-limiting biodegradation at the field scale. Their model incorporates effects of chemical and microbiological heterogeneities. The purpose of the modeling exercise was to investigate field-scale effective coefficients of retardation, dispersion, and decay of a soluble contaminant undergoing advection, sorption, and biodegradation in the subsurface. To simplify the analytical model, they assumed a steady-state microbial population; ignoring, thereby, the transient affects of microbial growth and perhaps more importantly the transient evolution of a contaminant plume that is in reality inextricably coupled to a dynamic microbial biomass plume. Miralles-Wilhelm et al. [54] concluded that the effective contaminant decay rate was less than the spatial mean.

Scholl [56] performed Monte Carlo simulations using the USGS model (BIOMOC) to study the effects of spatially distributed rates of biodegradation and hydraulic conductivity on plume-scale rates of biodegradation derived from field data. Three sets of simulations were performed, each involving 10 realizations, with different degrees of physical aquifer heterogeneity. Others used Monte Carlo analysis and Bayesian decision theory for assessing the effects of waste sites on groundwater quality [e.g. 20,41,42]. James and Freeze [62] developed a Bayesian decision framework for addressing questions of hydrogeological data worth associated with engineering design at sites in heterogeneous geological environments. They studied the specific case when one of remedial contaminant containment in an aquifer underlain by an aquitard of uncertain continuity. The framework is used to evaluate the worth of hard and soft data in investigating the aquitard's continuity. Similar to Miralles-Wilhelm et al. [54] study, Scholl [56] ignored biomass growth, death, and growth inhibition. Scholl calculated biodegradation rates from steady-state contaminant plumes using decrease in concentration down-gradient and a single flow velocity estimate; hence, the simulations performed did not reflect Monod kinetics or the transient changes of a contaminant plume that is coupled to a dynamic microbial biomass plume. Scholl [56] concluded for a steady-state contaminant plume that using an effective hydraulic conductivity/flow velocity and biomass distribution underestimates the time required to remediate a contaminated aquifer. Scholl did not investigate the affects of biological heterogeneity nor its correlations with spatial variations in aquifer permeability.

Three simulations (7–9) are performed; in which 250 different realizations of initial biomass concentration were enough to achieve stable mean discharges. For rational comparisons, the same initial total volumetric biomass is maintained in all simulations. In simulation 7, an ω of 0.2 is used to represent microbial characteristics or hydraulic conditions that limit microbial growth, while a higher value of 1.0 is used in simulations 8 and 9. The spatial log-variance (σ^2) of the initial biomass distribution is 1.0 in simulations 7 and 8 and 3 in simulation 9. For this reason, the biomass distribution in simulation 9 reflects the greatest range in bacterial concentrations (as depicted in Fig. 4 in [57]).

By comparing contaminant discharge curves for simulations 2 and 7 in Fig. 4 and or the time-integrated discharges in Table 2, it is evident that for low effective growth rates ($\omega \leq 0.2$), incipient biological heterogeneity does not significantly alter mass discharges at sections 1

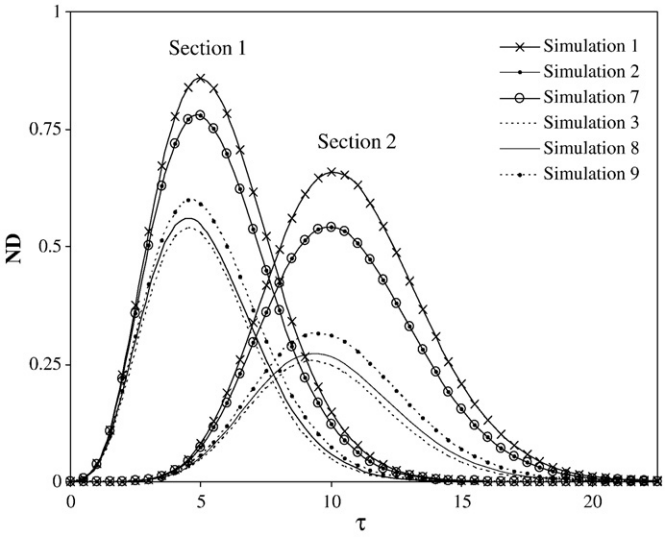

Fig. 4. Comparison between normalized mass discharge of homogenous simulations [1($\omega = 0.0$), 2($\omega = 0.2$) and 3($\omega = 1.0$)] and biological heterogeneity simulations [7($\omega = 0.2$, $\sigma_M^2 = 1.0$), 8($\omega = 1.0$, $\sigma_M^2 = 1.0$) and 9($\omega = 1.0$, $\sigma_M^2 = 3.0$)].

and 2 relative to the homogenous case. This suggests that a homogeneous aquifer assumption may in fact be sufficiently accurate for small ω values. In other words, for high flow velocities or low microbial activities, aquifers may be simulated as biologically homogeneous systems for the purpose of determining the contaminant mass discharge if critical electron donor/acceptors are not limiting. However, the uncertainty in the discharge prediction is not given from a deterministic homogeneous simulation. Fig. 4 also shows that when ω is increased to 1, as in simulation 8, contaminant attenuation is less efficient when the initial biomass distribution is non-uniform as oppose to being homogenous (simulation 3); which is consistent with finding of others [e.g. 55–57]. This means that the expected total mass passing sections 1 and 2 is higher in the heterogeneous case as shown in Table 3. Furthermore, attenuation decreases even more when the variance of the initial biomass distribution (σ^2) is increased as in simulation 9 (Fig. 4, Table 3). This is an outcome of the fact that increasing the incipient biomass distribution variance produces large regions where the initial biomass concentration is low and only small "islands" of large biomass concentrations. As a result, the contaminant plume escapes attenuation in large regions of low biomass, and because contaminant degradation and microbial growth are coupled, the absence of attenuation in these regions is not compensated by higher attenuation in other regions of greater biomass. For the highest value of ω considered in this work, simple calculations based on simulation output can show that maximum volume changes in biomass are several orders of magnitude smaller than initial pore space. As a consequence, effect of biomass clogging on porosity (and conductivity according to a model by Thullner et al. [109]) is found to be negligible. By comparing simulations 8 and 9 in Fig. 4 and Table 3 to the homogenous simulation 3, it is obvious that for high ω values, the assumption of a homogenous biomass distribution underestimates contaminant mass discharge. Because changes in mass discharges between the homogenous and biological heterogeneous systems are more apparent as the microbial effective growth rate (ω) increases, the estimation of ω is critical for predicting natural or induced bioattenuation.

4.3. Physical and biological heterogeneities

In this fourth scenario, correlated and uncorrelated biological and physical variability are considered. Brockman et al. [110] reported that it was indicated by different researchers that subsurface microbiological properties have similar spatial correlation length scales to those well established for subsurface physical and chemical parameters, and the microbiological properties appear to be spatially correlated to geologic, hydrologic and/or geochemical properties. This indicates that the possibility exists that the biological parameters (biomass distribution and electron done/acceptor) can have a spatial distribution and correlation structure similar to that of the hydraulic conductivity, K. It was also shown [111,112] that denitrification is highly variable and exhibits a distribution that is typically positively skewed and approximates the log-normal distribution. Brockman et al. [110] also indicate that if geologic or other physical properties in the subsurface control nutrient availability, spatial correlations between subsurface environmental and microbiological properties might be expected. Such correlation means that it is possible that the subsurface biological properties have similar variability structure to that of hydraulic conductivity.

Scheibe et al. [113] demonstrated that the widely observed decrease of the apparent rate of bacterial attachment (particularly as parameterized by the collision efficiency in filtration-based models) with transport distance could be interpreted as a field-scale manifestation of local-scale correlation between hydraulic conductivity variability and attachment rate coefficient variability. Because collision efficiency depends on properties of microbial cell surfaces [113], such dependency and the correlation to K imply that the biomass distribution in a heterogeneous aquifer may be related to hydraulic conductivity. Therefore, the spatial correlation structure of the hydraulic conductivity may have an imprint on the spatial structure of the biomass variability.

The above discussion indicates the possibility that biomass concentration and electron donors/acceptors may have similar spatial variability structure to that of hydraulic conductivity. However, there is no conclusive evidence in the literature substantiated by field data at the scale of interest in our study (focusing on engineering bioremediation applications) that supports or precludes this possibility. Thus, it is worth to examine the effects of the possible case that the biological parameters have spatial variation structure similar to that of K.

Additional six simulations (10–15) of 500 realizations each are considered in this scenario. In simulations 10 and 12 the two heterogeneities are assumed uncorrelated; while in simulations 11 and 13 they are assumed negatively correlated (Table 2). Negative correlations have been justified by others assuming that the high pore-water velocities, present in zones of high hydraulic conductivity regions, tend to wash out attached bacteria or precluded bacterial adhesion [114]. A positive correlation, on the other hand, has been justified assuming zones of high hydraulic conductivity facilitate the transport of nutrients necessary for microbial growth. The effect of a positive correlation between biological and physical heterogeneities is studied through simulations 14 and 15 (Table 2).

For simulations 10 and 11, a low effective growth rate ($\omega = 0.2$) is used. Looking at time-integrated contaminant discharges alone

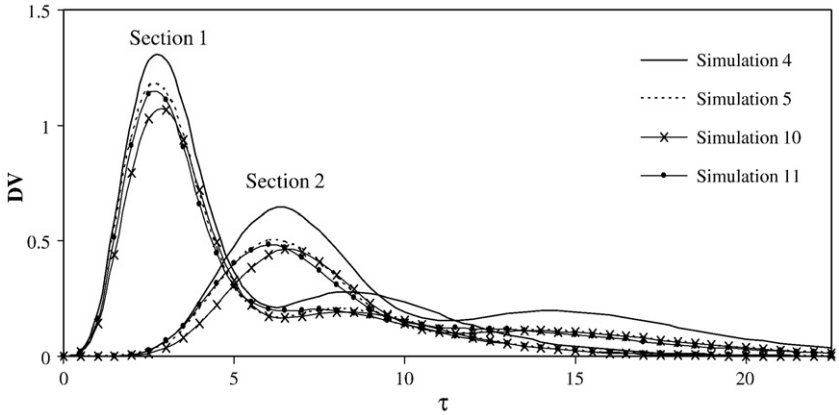

Fig. 5. Effect of −ve correlation between K and M for low ω (0.2) on discharge variance.

(Table 3), one surmises contaminant discharges are essentially the same as those generated under previous heterogeneous simulations 6 and 8 and homogeneous simulation 3. It appears again, low ω values determined by relatively high pore-water velocities or low maximum growth rates, define conditions for which non-uniform aquifer and biomass characteristics and their correlations can be effectively ignored if critical electron donors/acceptors are not limiting and the objective is to predict contaminant discharge but not its variance. With respect to discharge variance, a negative correlation between aquifer conducting and the incipient microbial biomass appears to increase discharge variance (or uncertainty) at the leading edge [see Fig. 5]. A negative correlation between K and microbial biomass produces flux variations at the leading edge that persist under low ω values. This occurs because initial microbial concentrations are lowest in the most permeable zones of the aquifer (which are also zones of high contaminant flux), and under low ω conditions, microbes are not growing fast enough to dampen spatial variations in contaminant flux.

In simulations 12, 13, and 14 ω is increased to 1. Results are comparable to those of heterogeneous simulations 6 and 8 and homogeneous simulation 3. In fact, results from Table 3 suggest contaminant discharge is insensitive to spatial correlations between aquifer conductivity and microbial biomass. The homogeneous simulation 3 over predicts attenuation by 10%; however, this error is well within the uncertainty of most contaminant transport models. Discharge variance appears to decrease at the first transect for MC simulation 13 where the correlation between aquifer conductivity and incipient microbial biomass concentrations is negative (see Fig. 6a). Conditions are more favorable for microbial growth/bioattenuation in this simulation than in 11, and in turn this growth has dampened spatial variations in contaminant flux. In fact, a closer examination of Fig. 6b suggests microbial growth may be obscuring much of the impact that initial biomass heterogeneities have on discharge variance; compare DV results of MC simulations 13 to 6 are almost identical at the first transect and in simulation 6 the initial biomass is spatially uniform. When the correlation is positive, higher concentrations of initial microbial biomass are located in higher contaminant flux zones and lower concentrations in lower flux zones. Discharge variances from positive and uncorrelated simulations 12 and 14 are almost indistinguishable which suggest DV is not dependent or less so when the correlation is positive. In MC simulation 15, the incipient biomass concentration variance is increased to 3.0. A comparison of this simulation and that of 9 shows the same level of contaminant attenuation irrespective of spatial correlations between varying parameters. The apparent loss of attenuation efficiency is due the high variance in the incipient biomass. In general, results suggest it may be difficult at best to discern the presence of positive or negative correlations between aquifer conductivity and microbial biomass from contaminant discharge alone. However, others have shown the effects of such correlations can be seen in plume concentration distributions [57].

4.4. Physical, chemical and biological heterogeneity

Chemical heterogeneity is examined in this last scenario. Several researchers studied this type of heterogeneity [115–119]. Li et al. [115,116] simulated reactive transport processes at the pore scale, accounting for heterogeneities of both physical and mineral properties. Mass balance principles were then used to calculate reaction rates at the continuum scale. In this final scenario the availability of the electron donor (ED)/acceptor (EA) which is crucial for the biodegradation is assumed to vary spatially. This assumption, which is justified by several researchers [e.g. 120–123], places additional constraints on where and at what rate contaminant attenuation occurs. With 500 realizations, only one MC simulation (16) is performed in which physical and biological heterogeneities are also considered. Similar to simulation 13, physical and biological heterogeneities are assumed to be negatively correlated; however, both are independent of the initial concentration distribution for the electron donor/acceptor. Also assumed is a unit microbial effective maximum growth rate and unit variances in the logarithms of hydraulic conductivity, incipient biomass concentration and incipient electron donor/acceptor concentrations.

Fig. 7a shows higher contaminant discharges in simulation 16, than in simulation 13; indicating that increasing system heterogeneity with respect to ED/EA variability reduces the efficiency of subsurface bioattenuation. This is because critical reaction processes became substrate-limited at multiple locations throughout the aquifer (as depicted in Fig. 9c in [57]). Table 3 suggests that cumulative attenuation

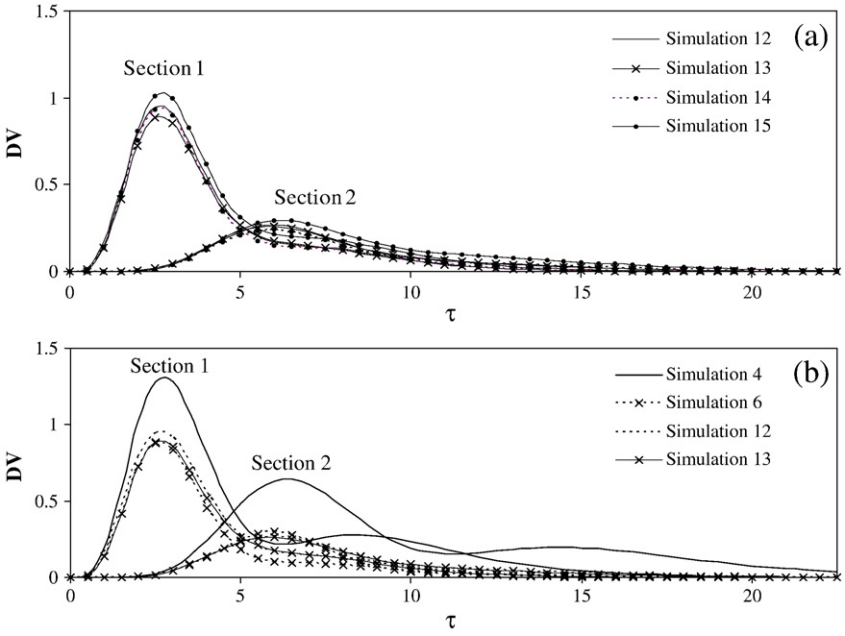

Fig. 6. Effect of correlation between K and M for high ω (1.0) in simulations 12 (no correlation, $\sigma_M^2 = 1.0$), 13 (negative correlation, $\sigma_M^2 = 1.0$), 14 (positive correlation, $\sigma_M^2 = 1.0$), and 15 (positive correlation, $\sigma_M^2 = 3.0$) on discharge variance.

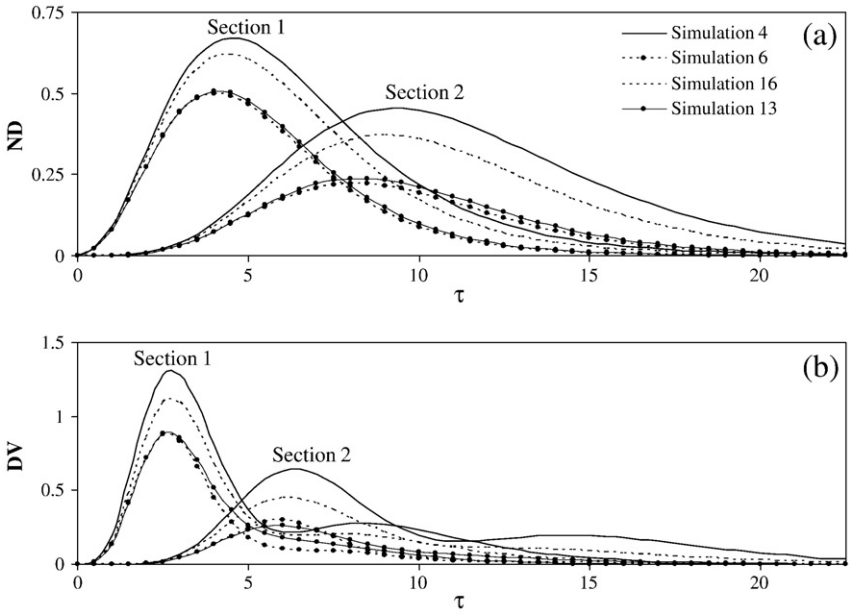

Fig. 7. Effect of electron donor/acceptor availability (a) normalized mean discharge, and (b) discharge variance.

efficiencies are most sensitive to ED/EA variability and the assumed concentration distribution for incipient biomass when groundwater velocity conditions favored microbial growth ($\omega \geq 1$) [see simulations 8, 9, 12, 13, 14, 15, and 16]. Only when ED/EA variability is considered, are noticeable changes to the cumulative discharge observed at both sections (compare simulations 3, 6, 13 and 16 in Table 3). This is consistent with the conclusions of Li et al. [115,116]. The spatial variability of ED/EA concentrations increases DV as well (Fig. 7b). That is the increase in ND for simulation 16 compared to simulation 13 is accompanied by an increase in DV. Hence, ignoring ED/EA variability can lead to an underestimation of the mass discharge and an underestimation of the uncertainty associated with that discharge.

5. Summary and conclusions

In this paper, Monte Carlo simulations were conducted to investigate spatial–temporal variations in subsurface microbial mediated contaminant discharge affected by a Damkohler number ω and physical, chemical, and biologically heterogeneities in a 2-D aquifer. Physical heterogeneity was represented as spatial variations in hydraulic conductivity. Biological heterogeneity was manifested as spatial variations in initial and transient distributions of microbial biomass, and finally chemical heterogeneity was included as spatial variations in the concentration of a requisite electron donor/acceptor. Monte Carlo simulations provided predictions for ensemble mean discharges at transects as well as the uncertainty in these predictions represented as discharge variances. Comparisons between Monte Carlo simulations and corresponding homogeneous scenarios of assumed uniform physical, chemical, and biological properties were used to elucidate the effects of physical, chemical, and biological heterogeneities and their possible correlation on contaminant mass discharges.

Physical heterogeneity increases dispersion in both longitudinal and transverse directions compared to homogenous simulations, which explained the early increase and the delayed decrease in ensemble mean contaminant discharges at model transects. The physical heterogeneities induced discharge variances at transects that varied over time; producing two peaks over time corresponding to two periods of high uncertainty in mass discharge. The first peak was observed to be associated with the arrival of the leading edge of the ensemble plume (i.e., when the steepest increase in mass discharge occurred), while the second occurred as the plume's trailing edge traverses the transect plane (i.e., when the steepest decrease in mass discharge occurred). A simple stream tube model was invoked to explain the occurrence of peaks in contaminant discharge variance.

Microbial mediated degradation decreased the expected contaminant mass discharge at a section transect and the discharge variance. The increasing microbial activity did not affect the arrival time of plumes in either homogenous or physically heterogeneous cases. A greater relative decrease in discharge variance occurred at the trailing edge of a simulated plume (second peak) than at the leading edge (first peak). This occurred most likely because the trailing edge encounters a higher density of active biomass produced as microbial growth increased to consume the leading edge of the plume, and also because the travel time and in turn the exposure to active microbial colonies was longer for contaminants in the trailing edge of plume.

When conditions were less favorable for microbial growth/attenuation ($\omega \leq 0.2$), the presence of physical heterogeneities and/or incipient biological heterogeneities did not significantly alter the contaminant mass discharge at a transect plane compared to predictions from deterministic homogenous simulations. This suggests that a homogeneous aquifer assumption may in fact be sufficiently accurate for small ω values. However, as growth conditions improved (ω increased) contaminant attenuation efficiency decreased significantly as the variations increased in the incipient biomass distribution. This was an outcome of the fact that increasing the biomass distribution variance produced large regions where initial biomass concentrations were low and only small “islands” of large biomass concentrations. As a result, the contaminant plume escaped attenuation in large regions of low biomass, and because contaminant degradation and microbial growth are coupled, the absence of attenuation in these regions was not compensated by higher attenuation in other regions of greater biomass.

The final MC simulation examined the sensitivity of contaminant discharge to spatial variations in the incipient concentrations of a critical electron donor/acceptor. The expected mass discharge and variance was quite sensitive to this particular chemical heterogeneity. More specifically, electron donor/acceptor variability produced significant reduction in subsurface bioattenuation efficiencies because critical reaction processes had become substrate-limited at locations throughout the aquifer. Expect contaminant discharges increased at

each transect as did discharge uncertainties. In general cumulative attenuation efficiencies were most sensitive to spatial variations in ED/EA and incipient biomass concentrations when conditions favored microbial growth ($\omega \geq 1.0$).

Acknowledgements

This research was partially funded by the Environmental Remediation Science Program (ERSP), U.S. Department of Energy: (Grant Number DE-FG02-08ER64585), the U.S. Department of Defense (project number ER0831) under the Environmental Security Technology Compliance Program (ESTCP), and the Research Affairs at the UAE University (project number 08-01-7-11/09).

References

[1] Basu NB, Rao PSC, Falta RW, Annable MD, Jawitz JW, Hatfield K. Temporal evolution of DNAPL source and contaminant discharge distribution: impacts of source mass depletion. J Contam Hydrol 2008;95(1–2):93–109.
[2] Einarson MD, Mackay DM. Predicting impacts of groundwater contamination. Environ Sci Technol 2001;35:66A–73A.
[3] Schwarz R, Ptak T, Holder T, Teutsch G. Groundwater risk assessment at contaminated sites: a new investigation approach. Groundwater quality: remediation and protection. Proceedings of the GQ'98 ConferenceTübingen, Germany: IAHS Publication; 1998. p. 49–55.
[4] Feenstra S, Cherry JA. Diagnosis and assessment of DNAPL sites. In: Pankow JF, Cherry JA, editors. Dense chlorinated solvents and other DNAPLs in groundwater. Portland, OR: Waterloo Press; 1996. p. 395–473.
[5] Hatfield K, Annable MD, Cho J, Rao PSC, Klammler H. A direct passive method for measuring water and contaminant fluxes in porous media. J Contam Hydrol 2004;75(3–4):155–81.
[6] Hatfield, K., Rao, P.S.C., Annable, M.D., Campbell T., 2002. Device and method for measuring fluid and solute fluxes in flow systems, Patent US 6, 402, 547 B1.
[7] Annable MD, Hatfield K, Cho J, Klammler H, Parker BL, Cherry JA, et al. Field-scale evaluation of the passive discharge meter for simultaneous measurement of groundwater and contaminant fluxes. Environ Sci Technol 2005;39(18): 7194–201.
[8] Basu NB, Rao PSC, Poyer IC, Annable MD, Hatfield K. Flux-based assessment at a manufacturing site contaminated with trichloroethylene. J Contam Hydrol 2006;86(1–2):105–27.
[9] Lee J, Rao PSC, Poyer IC, Toole RM, Annable MD, Hatfield K. Oxyanion discharge characterization using passive discharge meters: development and field testing of surfactant-modified granular activated carbon. J Contam Hydrol 2007;9, doi:10.1016/j.
[10] Bockelmann A, Ptak T, Teutsch G. An analytical quantification of mass fluxes and natural attenuation rate constants at a former gasworks site. J Contam Hydrol 2001;53(3–4):429–53.
[11] Bockelmann A, Zamfirescu D, Ptak T, Grathwohl P, Teutsch G. Quantification of mass fluxes and natural attenuation rates at an industrial site with limited monitoring network: a case study. J Contam Hydrol 2003;60(1–2):97–121.
[12] Bauer S, Bayer-Raich M, Holder T, Kolesar C, Muller D, Ptak T. Quantification of groundwater contamination in an urban area using integral pump tests. J Contam Hydrol 2004;75(3–4):183–213.
[13] Bayer-Raich M, Jarsjö J, Liedl R, Ptak T, Teutsch G. Average contaminant concentration and mass flow in aquifers from time dependent pumping well data: analytical framework. Water Resour Res 2004;40:W08303, doi:10.1029/2004WR003095.
[14] Bayer-Raich M, Jarsjö J, Liedl R, Ptak T, Teutsch G. Integral pumping test analysis of linearly sorbed groundwater contaminants using multiple wells: inferring mass flows and natural attenuation rates. Water Resour Res 2006;42:W08411, doi:10.1029/2005WR004244.
[15] Brooks MC, Wood L, Annable MD, Hatfield K, Cho J, Holbert C, et al. Changes in contaminant mass discharge from DNAPL source mass depletion: evaluation at two field sites. J Contam Hydrol 2008;102:140–53.
[16] Rao PSC, Jawitz JW, Enfield CG, Falta RW, Annable MD, Wood AL. Technology integration for contaminated site remediation: cleanup goals and performance criteria. In: Thornton SF, Oswald SE, editors. Groundwater quality: natural and enhanced restoration of groundwater pollution. Sheffield, UK: IAHS Press; 2002. p. 571–8.
[17] Enfield CG, Wood AL, Brooks MC, Annable MD. Interpreting tracer data to forecast remedial performance. In: Thornton SF, Oswald SE, editors. Groundwater quality: natural and enhanced restoration of groundwater pollution. Sheffield, UK: IAHS Press; 2002. p. 11–6.
[18] Enfield CG, Wood AL, Espinoza FP, Brooks MC, Annable M, Rao PSC. Design of aquifer remediation systems: (1) describing hydraulic structure and NAPL architecture using tracers. J Contam Hydrol 2005;81(1–4):125–47.
[19] Rao PSC, Jawitz JW. Comment on "Steady state mass transfer from single-component dense nonaqueous phase liquids in uniform flow fields" by T.C. Sale and D.B. McWhorter. Water Resour Res 2003;39(3):1068.
[20] Parker JC, Park E. Modeling field-scale dense nonaqueous phase liquid dissolution kinetics in heterogeneous aquifers. Water Resour Res 2004;40:W05109, doi:10.1029/2003WR002807.
[21] Zhu J, Sykes JF. Simple screening models of NAPL dissolution in the subsurface. J Contam Hydrol 2004;72(1–4):245–58.
[22] Falta RW, Rao PSC, Basu N. Assessing the impacts of partial mass depletion in DNAPL source zones: I. Analytical modeling of source strength functions and plume response. J Contam Hydrol 2005;78(4):259–80.
[23] Falta RW, Rao PSC, Basu N. Assessing impacts of partial mass depletion in DNAPL source zones: II. Coupling source strength functions to plume evolution. J Contam Hydrol 2005;79(1–2):45–66.
[24] Jawitz JW, Fure AD, Demy GG, Berglund S, Rao PSC. Groundwater contaminant discharge reduction resulting from nonaqueous phase liquid mass reduction. Water Resour Res 2005;41, doi:10.1029/2004WR003825.
[25] Park E, Parker JC. Evaluation of an upscaled model for DNAPL dissolution kinetics in heterogeneous aquifers. Adv Water Resour 2005;28(12):1280–91.
[26] Fure AD, Jawitz JW, Annable MD. DNAPL source depletion: linking architecture and discharge response. J Contam Hydrol 2006;85(3–4):118–40.
[27] Christ JA, Ramsburg CA, Pennell KD, Abriola LM. Estimating mass discharge from dense nonaqueous phase liquid source zones using upscaled mass transfer coefficients: an evaluation using multiphase numerical simulations. Water Resour Res 2006;42:W11420, doi:10.1029/2006WR004886.
[28] McGuire TM, McDade JM, Newell CJ. Performance of DNAPL source depletion technologies at 59 chlorinated solvent-impacted sites. Ground Water Monit Remediat 2006;26(1):73–84.
[29] Gelhar LW, Gutjahr AL, Naff RL. Stochastic analysis of macrodispersion in a stratified aquifer. Water Resour Res 1979;15(6):1387–97.
[30] Gelhar LW, Axness CL. Three-dimensional stochastic analysis of macrodispersion in aquifers. Water Resour Res 1983;19(1):161–80.
[31] Dagan G. Solute transport in heterogeneous porous formations. J Fluid Mech 1984;145:151–77.
[32] Dagan G. Time-dependent macrodispersion for solute transport in anisotropic heterogeneous aquifers. Water Resour Res 1988;24(90):1491–500.
[33] Kabala ZJ, Sposito G. A stochastic model of reactive solute transport with time-varying velocity in a heterogeneous aquifer. Water Resour Res 1991;27(3):341–50.
[34] Kabala ZJ, Sposito G. Statistical moments of reactive solute concentration in a heterogeneous aquifer. Water Resour Res 1994;30(3):759–68.
[35] Cvetkovic VD, Shapiro AM. Mass arrival of sorptive solute in heterogeneous porous media. Water Resour Res 1990;26(9):2057–67.
[36] Cvetkovic VD, Dagan G, Cheng H. Contaminant transport in aquifers with spatially variable hydraulic and sorption properties. Proc R Soc London Ser A 1998;454:2173–207.
[37] Dagan G, Cvetkovic VD. Spatial moments of a kinetically sorbing solute plume in a heterogeneous aquifer. Water Resour Res 1993;29(12):4053–61.
[38] Vert M, Ptak T, Biver P, Vittori J. Geostatistical generation of three-dimensional aquifer realizations using the conditional SIS approach with direction trends imposed on variogram models. In: Gomez-Hernandez JJ, et al, editor. geoENV II—geostatistics for environmental applications. Dordrecht: Kluwer Academic; 1999. p. 343–54.
[39] Dagan G. Flow and transport in porous formations. Berlin: Springer; 1989.
[40] Ptak T, Teutsch G. Macrodispersivity in highly heterogeneous porous aquifers. In: Hötzl H, Werner A, editors. Tracer hydrology. Rotterdam: Balkema; 1992. p. 149–55.
[41] Gelhar LW. Stochastic subsurface hydrology from theory to applications. Water Resour Res 1986;22(9):135–45.
[42] Gelhar LW. Stochastic subsurface hydrology. Prentice Hall: Englewood Cliffs; 1993.
[43] Bellin A, Rinaldo A, Bosma WJP, van der Zee SM, Rubin Y. Linear equilibrium adsorbing solute transport in physically and chemically heterogeneous porous formations, 1: analytical solutions. Water Resour Res 1993;29(12):4019–30.
[44] Burr DT, Sudicky EA, Naff RL. Non-reactive and reactive solute transport in three-dimensional heterogeneous porous media: mean displacement, plume spreading, and uncertainty. Water Resour Res 1994;30(3):791–815.
[45] Hu BX, Cushman JH, Deng FW. Nonlocal reactive transport with physical, chemical, and biological heterogeneity. Adv Water Resour 1997;20(5–6): 293–308.
[46] Hu BX, Deng FW, Cushman JH. Nonlocal reactive transport with physical and chemical heterogeneity: linear nonequilibrium sorption with random Kd. Water Resour Res 1995;31(9):2239–52.
[47] Valocchi AJ. Spatial moment analysis of the transport of kinetically adsorbing solutes through stratified aquifers. Water Resour Res 1989;25(2):273–9.
[48] Grathwohl P, Kleineidam S. Impact of heterogeneous aquifer materials on sorption capacities and sorption dynamics of organic contaminants. Groundwater quality: remediation and protection. IAHS Publ 1995;225:79–86.
[49] Ptak T, Strobel H. Sorption of fluorescent tracers in a physically and chemically heterogeneous aquifer material. In: Arehart GB, Hulston JR, editors. Water–rock interaction. Rotterdam: Balkema; 1998. p. 177–80.
[50] Karapanagioti HK, Sabatini DA, Kleineidam S, Grathwohl P, Ligouis B. Phenanthrene sorption with heterogeneous organic matter in a landfill aquifer material. Phys Chem Earth Bio 1999;24(6):535–41.
[51] Kleineidam S, Rügner H, Grathwohl P. Impact of grain scale heterogeneity on slow sorption kinetics. Environ Toxic Chem 1999;18(8):1673–8.
[52] Rügner H, Kleineidam S, Grathwohl P. Long term sorption kinetics of phenanthrene in aquifer materials. Environ Sci Technol 1999;33(10):1645–51.
[53] Ptak T, Schmid G. Dual-tracer transport experiments in a physically and chemically heterogeneous porous aquifer: effective transport parameters and spatial variability. J Hydrol 1996;183(1–2):117–38.

[54] Miralles-Wilhelm F, Gelhar LW, Kapoor V. Stochastic analysis of oxygen-limited biodegradation in three-dimensionally heterogeneous aquifers. Water Resour Res 1997;33(6):1251–63.
[55] Miralles-Wilhelm F, Gelhar LW. Stochastic analysis of oxygen-limited biodegradation in heterogeneous aquifers with transient microbial dynamics. J Contam Hydrol 2000;42:69–97.
[56] Scholl MA. Effects of heterogeneity in aquifer permeability and biomass on biodegradation rate calculations—results from numerical simulations. Ground Water 2000;38(5):702–12.
[57] Mohamed MAM, Hatfield K, Hassan AE. Monte Carlo evaluation of microbial-mediated contaminant reactions in heterogeneous aquifers. Adv Water Resour 2006;29:1123–39.
[58] Chaudhuri A, Sekhar M. Stochastic finite element method for analysis of transport of nonlinearly sorbing solutes in three-dimensional heterogeneous porous media. Water Resour Res 2007;43:W07442, doi:10.1029/2006WR004892.
[59] Marin CM, Medina Jr MA, Butcher JB. Monte Carlo analysis and Bayesian decision theory for assessing the effects of waste sites on groundwater: I. Theory. J Contam Hydrol 1989;5:1–13.
[60] Medina Jr MA, Butcher JB, Marin CM. Monte Carlo analysis and Bayesian decision theory for assessing the effects of waste sites on groundwater: II. Applications. J Contam Hydrol 1989;5:15–31.
[61] Chaudhuri A, Sekhar M. Analysis of biodegradation in a 3-D heterogeneous porous medium using nonlinear stochastic finite element method. Adv Water Resour 2007;30(3):589–605.
[62] James BR, Freeze RA. The worth of data in predicting aquitard continuity in hydrogeological design. Water Resour Res 1993;29(7):2049–65.
[63] Dagan G. Transport in heterogeneous porous formations — spatial moments, ergodicity, and effective dispersion. Water Resour Res 1990;26(6):1281–90.
[64] Dagan G, Fiori A. The influence of pore-scale dispersion on concentration statistical moments in transport through heterogeneous aquifers. Water Resour Res 1997;33(7):1595–605.
[65] Fiori A, Berglund S, Cvetkovic V, Dagan G. A first-order analysis of solute discharge statistics in aquifers: the combined effect of pore-scale dispersion, sampling, and linear sorption kinetics. Water Resour Res 2002;38(8):1137 [Art].
[66] Rubin Y. Prediction of tracer plume migration in disordered porous media by the method of conditional probabilities. Water Resour Res 1991;27(6):1291–308.
[67] Curtis GP, Roberts PV, Reinhard M. A natural gradient experiment on solute transport in a sand aquifer, 4, sorption of organic solutes and its influence on mobility. Water Resour Res 1986;22(13):2059–68.
[68] Mackay DM, Freyberg DL, Roberts PV, Cherry JA. A natural gradient experiment on solute transport in a sand aquifer, 1, approach and overview of plume movement. Water Resour Res 1986;22(13):2017–29.
[69] Freyberg DL. A natural gradient experiment on solute transport in a sand aquifer, 2, spatial moments and the advection and dispersion of nonreactive tracers. Water Resour Res 1986;22(13):2031–46.
[70] Deng F-W, Cushman JH, Delleur JW. A Fast Fourier transform stochastic analysis of the contaminant transport problem. Water Resour Res 1993;29(9):3241–7.
[71] LeBlanc DR, Garabedian SP, Hess KH, Gelhar LW, Quadri RD, Stollenwerk KG, et al. Large-scale natural gradient tracer test in sand and gravel, Cape Cod, Massachusetts, 1, experimental design and observed tracer movement. Water Resour Res 1991;27(5):895–910.
[72] Barry DA, Coves J, Sposito G. On the Dagan model of solute transport in groundwater: application to the Borden site. Water Resour Res 1988;24(10):1805–17.
[73] Bailey JE, Ollis DF. Biochemical engineering fundamentals. New York: McGraw Hill; 1977.
[74] Molz FJ, Widdowson MA, Benefield LD. Simulation of microbial growth dynamics coupled to nutrient and oxygen transport in porous media. Water Resour Res 1986;22(8):1207–16.
[75] Rittmann BE, McCarty PL, Roberts PV. Trace-organics biodegradation in aquifer recharge. Ground Water 1980;18:236–43.
[76] Bouwer EJ, McCarty PL. Modeling of trace organics biotransformation in the subsurface. Ground Water 1984;22:433–40.
[77] Bouwer EJ, Cobb GD. Modeling of biological processes in the subsurface. Water Sci Technol 1987;19:769–79.
[78] Champagne P, Parker WJ, Van-Geel P. Modeling cometabolic biodegradation of organic compounds in biofilms. Water Sci Technol 1999;39(7):147–52.
[79] Långmark J, Storeya MV, Ashboltb NJ, Stenström TA. Artificial groundwater treatment: biofilm activity and organic carbon removal performance. Water Res 2004;38(3):740–8.
[80] Kim H, Jaffé Peter R, Young Lily Y. Simulating biodegradation of toluene in sand column experiments at the macroscopic and pore-level scale for aerobic and denitrifying conditions. Adv Water Resour 2004;27(4):335–48.
[81] Iliuta I, Larachi F. Modeling simultaneous biological clogging and physical plugging in trickle-bed bioreactors for wastewater treatment. Chem Eng Sci 2005;60(5):1477–89.
[82] Liang C, Chiang P, Chang E. Modeling the behaviors of adsorption and biodegradation in biological activated carbon filters. Water Res 2007;41(15):3241–50.
[83] Liang C, Chiang P. Mathematical model of the non-steady-state adsorption and biodegradation capacities of BAC filters. J Hazar Mater 2007;139(2):316–22.
[84] Simpson DR. Biofilm processes in biologically active carbon water purification. Water Res 2008;42(13):2839–48.
[85] Buchanan W, Roddicka F, Porter N. Removal of VUV pre-treated natural organic matter by biologically activated carbon columns. Water Res 2008;42(13):3335–42.
[86] Watson JE, Gardner WR. A mechanistic model of bacterial colony growth response to substrate supply. A paper presented at the Chapman Conference on Microbial Processes in the Transport, Fate, and In Situ Treatment of Subsurface Contaminants. Snowbird, UT; 1986.
[87] Yoshida H, Yamamoto K, Yogo S, Murakami Y. An analogue of matrix diffusion enhanced by biogenic redox reaction in fractured sedimentary rock. J Geochem Explor 2006;90(1–2):134–42.
[88] Bazin MJ, Saunders PT, Prosser JI. Models of microbial interactions in the soil. CRC Crit Rev Microbiol 1976;4:463–98.
[89] Corapcioglu MY, Haridas A. Transport and fate of microorganisms in porous media: a theoretical investigation. J Hydrol 1984;72:149–69.
[90] Corapcioglu MY, Haridas A. Microbial transport in soils and groundwater: a numerical model. Adv Water Resour 1985;8:188–200.
[91] Borden RC, Bedient PB. Transport of dissolved hydrocarbons influenced by oxygen-limited biodegradation: 1. Theoretical Development. Water Resour Res 1986;22(13):1973–82.
[92] Celia MA, Kindred JS. Numerical simulation of subsurface contaminant transport with multiple nutrient biodegradation. Proceedings of the International Conference on the Impact of Physiochemistry on the Study, Design, and Optimization of Processes in Natural Porous Media. Nancy, France: Presses University de Nancy; 1987.
[93] Bauer RD, Maloszewski P, Zhang Y, Meckenstock RU, Griebler C. Mixing-controlled biodegradation in a toluene plume—results from two-dimensional laboratory experiments. J Contam Hydrol 2008;96(1–4):150–68.
[94] Baveye P, Valocchi A. An evaluation of mathematical models of the transport of biologically reacting solutes in saturated soils and aquifers. Water Resour Res 1989;25(6):1413–21.
[95] MacQuarrie KTB, Sudicky EA, Frind EO. Simulation of biodegradable organic contaminants in groundwater 1. Numerical formulation in principal directions. Water Res Res 1990;26(2):207–17.
[96] Chiang CY, Dawson CN, Wheeler MF. Modeling of in-situ biorestoration of organic compounds in groundwater, technical report. Trans porous media 1991;6:667–702.
[97] Andricevic R, Cvetkovic V. Evaluation from contaminants migrating by groundwater. Water Resour Res 1996;32(3):611–21.
[98] Maxwell RM, Kastenberg WE. Stochastic environmental risk analysis: an integrated methodology for predicting risk from contaminated groundwater. Stoch Env Res Risk Assess 1999;13:27–47.
[99] Hassan AE, Cushman JH, Delleur JW. Monte Carlo studies of flow and transport in fractal conductivity fields: comparison with stochastic perturbation theory. Water Resour Res 1997;33(11):2519–34.
[100] Hassan AE, Cushman JH, Delleur JW. A Monte Carlo assessment of Eulerian flow and transport perturbation models. Water Resour Res 1998;34(5):1143–63.
[101] Mohamed MAM. METABIOTRANS: A finite element model for metals transport and biotransformation in saturated groundwater, Ph.D. Dissertation, University of Florida, USA, 2001.
[102] Mohamed MM, Hatfield K, Perminova IV. Evaluation of Monod kinetic parameters in the subsurface using moment analysis: theory and numerical testing. Adv Water Resour 2007;30:2034–50.
[103] Kindred JS, Celia MA. Contaminant transport and biodegradation 2: conceptual model and test simulation. Water Resour Res 1989;25:1149–59.
[104] Schafer D, Schafer W, Kinzelbach W. Simulation of reactive processes related to biodegradation in aquifers: 1. Structure of the three-dimensional reactive transport model. J Contamin Hydrol 1998;31(1–2):167–86.
[105] Brusseau M, Xie L, Li L. Biodegradation during contaminant transport in porous media: 1. Mathematical analysis of controlling factors. J Contamin Hydrol 1999;37:269–93.
[106] Isaaks, Srivastava. An introduction to applied geostatistics. Oxford University Press; 1989. p. 486.
[107] Rifai HS, Bedient PB. Comparison of biodegradation kinetics with an instantaneous reaction model for groundwater. Water Resour Res 1990;26:637–45.
[108] Rashid M, Kaluarachchi J. A simplified numerical algorithm for oxygen- and nitrate-based biodegradation of hydrocarbons using Monod expressions. J Contam Hydrol 1999;40(1):53–77.
[109] Thullner M, Schroth MH, Zeyer J, Kinzelbach W. Modeling of a microbial growth experiment with bioclogging in a two-dimensional saturated porous media flow field. J Contam Hydrol 2004;70:37–62.
[110] Brockman FJ, Christopher JM. Subsurface microbiological heterogeneity: current knowledge, descriptive approaches and applications. FEMS Microbiol Rev 1997;20:231–47.
[111] Parkin TB. Soil microsites as a source of denitrification variability. Soil Sci Soc Am 1987;51:1194–9.
[112] Parkin RB, Robinson JA. Stochastic models of soil denitrification. Appl Environ Microbiol 1989;55:72–7.
[113] Scheibe TD, Dong H, Xie Y. Correlation between bacterial attachment rate coefficients and hydraulic conductivity and its effect on field-scale bacterial transport. Adv Water Resour 2007;30:1571–82.
[114] Murphy EM, Ginn TR, Chilakapti A, Reseh CT, Phillips JL, Wietsma TW, et al. The influence of physical heterogeneity on microbial degradation and distribution in porous media. Water Resour Res 1997;33(5):1087–103.
[115] Li L, Peters CA, Celia MA. Upscaling geochemical reaction rates using pore-scale network modeling. Adv Water Resour 2006;29(9):1351–70.
[116] Li L, Peters CA, Celia MA. Applicability of averaged concentrations in determining geochemical reaction rates in heterogeneous porous media. Am J Sci 2007;307:1146–66.

[117] Glassley WE, Simmons AM, Kercher JR. Mineralogical heterogeneity in fractured, porous media and its representation in reactive transport models. Appl Geochem 2002;17(6):699–708.
[118] Scheibe TD, Fang Y, Murray CJ, Roden EE, Chen J, Chien Y. Transport and biogeochemical reaction of metals in a physically and chemically heterogeneous aquifer. Geosphere 2006;2(4), doi:10.1130/GES00029.1.
[119] Tompson AFB, Schafer AL, Smith RW. Impacts of physical and chemical heterogeneity on cocontaminant transport in a sandy porous medium. Water Resour Res 1996;32(4):801–18.
[120] Lovley DR, Coates JD, Blunt-Harris EL, Phillips EJP, Woodward JC. Humic substances as electron acceptors for microbial respiration. Nature 1996;382: 445–8.
[121] Lovley DR, Fraga JL, Coates JD, Blunt-Harris EL. Humics as an electron donor for anaerobic respiration. Environ Microbiol 1999;1:89–98.
[122] Gu BH, Chen J. Enhanced microbial reduction of contaminant and U(VI) by different natural organic matter fractions. Geochim Cosmochim Acta 2003;67:3575–82.
[123] Perminova IV, Hatfield K. Remediation chemistry of humic substances: theory and implications for technology. In: Use of humic substances to remediate polluted environments: from theory to practice. In: Perminova IV, Hatfield K, Hertkorn N, editors. NATO Science Series: IV: Earth and Environmental Sciences, Vol. 52. Springer; 2005. p. 3–36.